Physica C 168 (1990) 571–579
North-Holland

FORMATION OF THEORETICAL-DENSITY MICROHOMOGENEOUS $YBa_2Cu_3O_{7-x}$ USING A MICROEMULSION-MEDIATED PROCESS

Pushnan AYYUB [1], A.N MAITRA [2] and D.O. SHAH [3]

Center for Surface Science and Engineering, Department of Chemical Engineering, University of Florida, Gainesville, Florida 32611, USA

Received 26 February 1990
Revised manuscript received 14 May 1990

We describe a new technique using microemulsions for synthesizing an ultra-homogeneous, microparticulate precursor for the production of sintered $YBa_2Cu_3O_{7-x}$. The process ensures a uniform mixing of the cations down to a scale of at least 10 nm. The finely dispersed oxalate precursor (particle size ≈ 50 nm) yields single-phase $YBa_2Cu_3O_{7-x}$ powder (particle size ≈ 275 nm) on calcining at 820°C. The material sintered at 925°C has a very compact microstructure with large (15–50 μm) grains and has a bulk density that is about 98% of the theoretical (single-crystal) value. It also exhibits a significantly higher Meissner effect than the material produced by conventional aqueous precipitation when both are sintered under identical conditions.

1. Introduction

It is now recognized that many of the properties of the recently-discovered oxide superconductors are critically dependent on the microstructure. A desired microstructure may be obtained by controlling the morphology and size-distribution of the precursor (uncalcined powder) and optimizing the sintering conditions. As sintering is promoted by a decreasing surface free energy, a uniform *microparticulate* precursor is essential for obtaining high-density sintered material. Conventional solid state reaction (involving the oxides or carbonates of Y, Ba and Cu) yields $YBa_2Cu_3O_{7-x}$ (YBCO) ceramic with large particles and a wide distribution of sizes and is unsuitable for sintering. In principle it is possible to produce a homogeneous, fine-grained powder using co-precipitation methods. However, in the case of YBCO, it is very difficult to achieve strictly simultaneous precipitation due to the dissimilar chemistry of Y, Ba and Cu salts. Also, during a chemical reaction in a bulk aqueous medium, the nucleation and the subsequent growth of the precipitated particles occur in an uncontrolled manner. These problems can be avoided by using the microemulsion as a reaction medium.

A microemulsion is generally defined as a thermodynamically stable, optically isotropic dispersion of aqueous and hydrocarbon phases in the presence of at least one species of surface-active (surfactant) molecules [1,2]. For the present, we are interested in systems in which the aqueous phase is dispersed as microdroplets surrounded by a monolayer of surfactant molecules in the continuous hydrocarbon phase (water-in-oil microemulsions). The dimension of the water droplets is typically between 10 and 50 nm, depending on the nature and proportion of the constituents. If a soluble metal salt is incorporated in the aqueous phase of the microemulsion then it will reside within isolated droplets (10–50 nm in size) surrounded by oil. The microdispersed metal salt may subsequently be reduced or oxidized to produce metal or metal oxide microparticles. Water-in-oil microemulsions have been used to synthesize col-

[1] Present and permanent address: Materials Science Group, Tata Institute of Fundamental Research, Homi Bhabha Road, Bombay 400 005, India.

[2] Present and permanent address: Department of Chemistry, University of Delhi, New Delhi 110 007, India.

[3] Also: Department of Anesthesiology, University of Florida, Gainesville, FL 32611, USA.

0921-4534/90/$03.50

loidal metals [3], colloidal Fe_3O_4 [4], colloidal AgCl [5] and microcrystalline Fe_2O_3 [6].

2. Characterization of the microemulsion

We selected a microemulsion with the following four components: cetyltrimethylammonium bromide (surfactant, also known as CTAB), 1-butanol (co-surfactant), n-octane (which constitutes the continuous hydrocarbon phase) and the aqueous phase. The CTAB:butanol ratio was kept fixed at 1:0.73 during the determination of the phase diagram and subsequent experiments. The pseudo-three-component phase diagram of this system (for the case where pure water constitutes the aqueous phase) is shown in fig. 1. L_2 and L_1 represent the isotropic one-phase water-in-oil and oil-in-water regions, respectively, while the intermediate grey area represents a birefringent phase. Figure 2 depicts the phase diagram of the system in which the aqueous phase consists of a mixture of the nitrates of Y, Ba and Cu, the concentrations of the metal ions being 0.05, 0.10 and 0.15 M/l, respectively. To avoid errors due to an uncertainty in the water of crystallization associated with $Y(NO_3)_3$ and $Cu(NO_3)_2$, the starting solution was produced by dissolving Y_2O_3 and CuO in hot concentrated nitric acid and later adding $Ba(NO_3)_2$. The metal salts (from Aldrich) were at least 99.9% pure. CTAB (99%) was obtained from Sigma, while butanol (99.8%) and octane (reagent grade) were obtained from Fisher Scientific. Water was deionized and distilled before use.

It is apparent from fig. 2 that the CTAB/butanol/octane system solubilizes a relatively large proportion of the aqueous nitrate solution producing a stable, transparent and homogeneous phase (the large unshaded domain to the right of the diagram). The microstructure of this phase was investigated by electrical conductivity and bulk viscosity measurements (fig. 3). These measurements were made as a function of increasing aqueous phase fraction (with constant surfactant/co-surfactant/oil ratio), corresponding to a movement along the straight line from

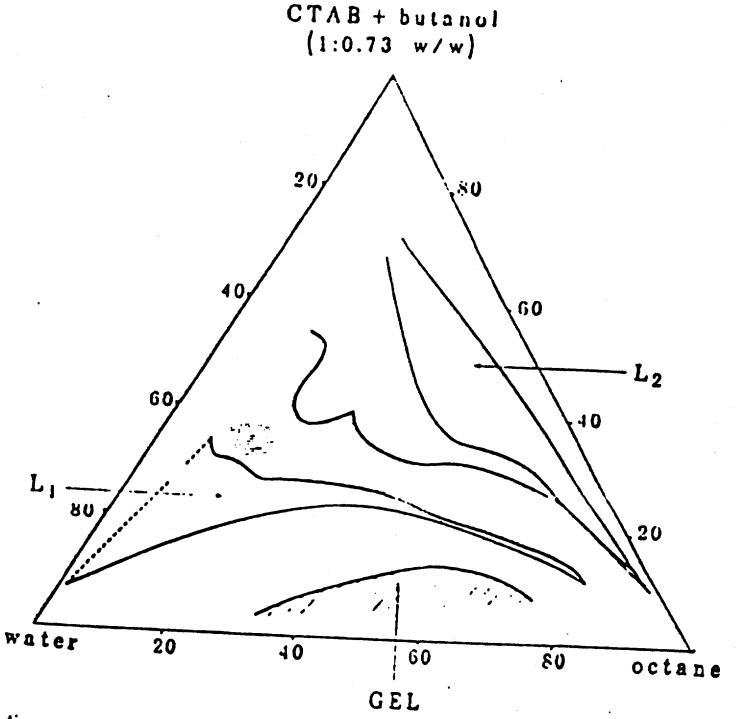

Fig. 1. Pseudoternary phase diagram (at 25°C) of the (CTAB + butanol)/octane/water system. The boundaries of the water-in-oil (L_2) and oil-in-water (L_1) regions are shown. The intermediate shaded zone represents an optically anisotropic phase.

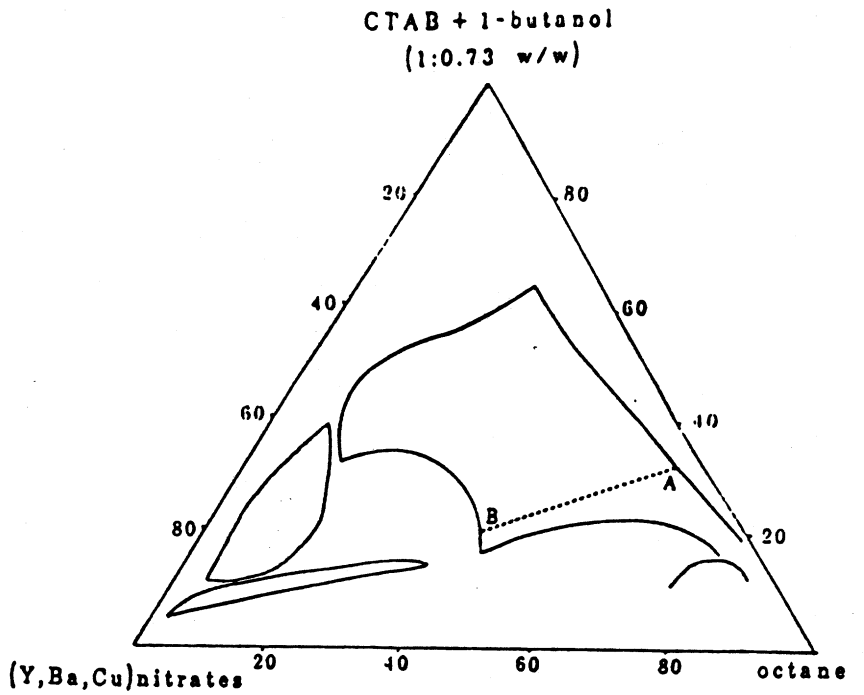

Fig. 2. Pseudoternary phase diagram of the (CTAB + butanol)/octane/(Y, Ba, Cu) nitrate solution system (at 25 °C).

A to B in fig. 2. In a random system consisting of conducting droplets dispersed in an insulating medium, the conductivity should increase with the aqueous phase fraction $f(w)$, until percolation occurs. The percolation threshold is lowered in the presence of an attractive inter-droplet interaction [7]. The presence of such an interaction is also reflected in the bulk viscosity of the system. A study of the optical properties of the system confirms that the sharply rising portion (i.e. below $f(w) \approx 15\%$) of the conductivity and viscosity curves actually corresponds to the water-in-oil (inverted micelle) type of microstructure. The fluid microstructure corresponding to higher values of $f(w)$ is expected to be more complicated and cannot be accurately characterized with the help of the techniques used in the present study. A more detailed study of the physicochemical properties of the CTAB/butanol/octane/(aqueous solution) system and the effects of added salts will be reported separately [8].

3. Microemulsion reaction vis-a-vis bulk aqueous reaction

The composition of the microemulsions used for the synthesis of YBCO are given in table 1. The aqueous phase fraction was kept fixed at 11.3% (note that this is well below the comparatively flat portion of the conductivity and viscosity curves and should therefore correspond to the water-in-oil type of microstructure). The hydrodynamic diameter, D_h, of the microemulsion droplets was determined from a measurement of the time decay of the intensity autocorrelation function obtained from quasi-elastic light scattering [9]. The $Cu(NO_3)_2$ in the aqueous phase strongly absorbs the blue-green Ar-laser lines leading to unreliable results. D_h was therefore measured for a system having the same composition as "1" (see table 1), except that the aqueous phase contained only $Y(NO_3)_3$. For this system: $D_h = 13.0 \pm 0.5$ nm.

Chemical reaction between the metal salts and ammonium oxalate (precipitating agent) is achieved by the gradual addition of the microemulsion "1" to

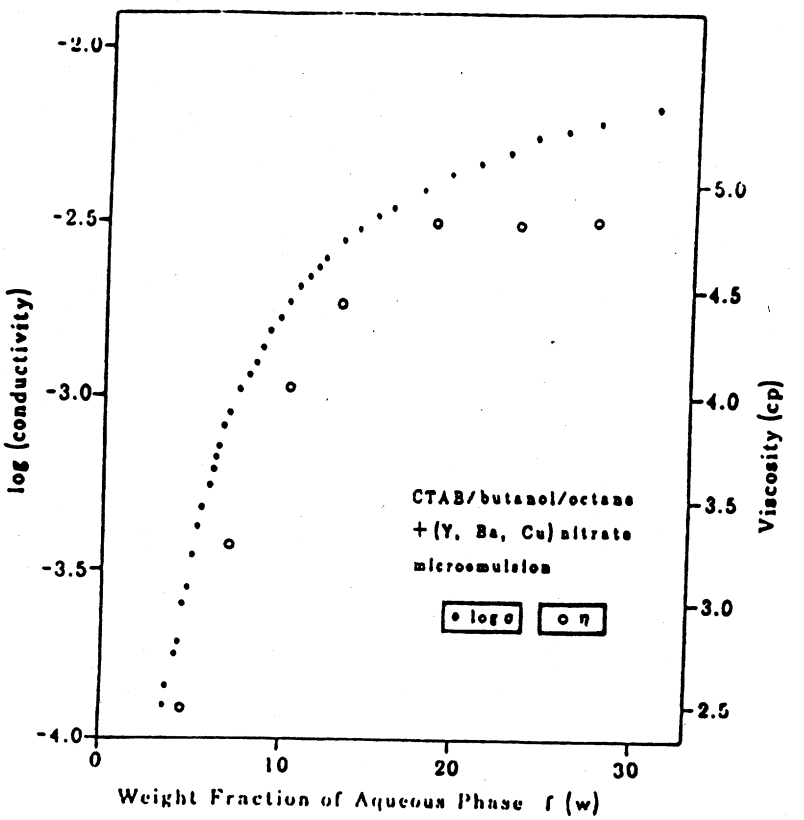

Fig. 3. Variation of the electrical conductivity (at 60 Hz) and bulk viscosity of the (CTAB+butanol)/octane/(Y, Ba, Cu) nitrate solution system with the weight fraction of the aqueous phase. Both the measurements were made at 25°C.

Table I
Composition of the microemulsions used for chemical reactions.

	Surfactant phase	Hydrocarbon phase	Aqueous phase
Microemulsion I	CTAB + 1-butanol	n-octane	(Y, Ba, Cu) nitrate solution, Total metal concentration = 0.3 N
Microemulsion II	CTAB + 1-butanol	n-octane	Ammonium oxalate solution, Concentration = 0.45 N
Weight fraction (for both "I" and "II")	29.25%	59.42%	11.33%

Note: CTAB = Cetyltrimethylammonium bromide.

"II". The aqueous cores of the water-in-oil microemulsion frequently colloide and move apart rapidly [10]. This allows the reacting species to come into contact when "I" and "II" are mixed. Since the two systems ("I" and "II") have the same surfactant:hydrocarbon:aqueous phase ratio (differing only in the nature of the salt dissolved in the water), the microemulsion phase does not get destabilized on mixing them. The steric barrier provided by the surfactant monolayer restricts the growth of the precipitated oxalate particles and hinders intergrain coagulation. Serial precipitation of the cations (which may occur in conventional wet methods) is avoided in the present approach: the upper limit to the scale

of chemical inhomogeneity being set by the dimension of the "microreactors"-about 13 nm in the present case. The (Y, Ba, Cu) oxalate precipitate was separated from the oil and surfactant by centrifuging and washing with a 1:1 mixture of methanol and chroloform, followed by ethanol. Once the surfactant is washed off, interparticle coagulation occurs to some extent – presumably during the extraction and drying of the precipitate. However, the precipitated oxalate particles produced by this method are still substantially smaller than those produced by conventional bulk precipitation (see table II).

To ascertain the efficacy of this method, we made a parallel study of the precipitation of the (Y, Ba, Cu) oxalates in an unconstrained aqueous medium. The concentration of the reactants was the same as in "I" and "II". The reaction pH was kept constant at predetermined values while the metal nitrates were gradually added to ammonium oxalate. The precipitate yield was measured at each pH value and has been plotted as a fraction of the expected yield (assuming complete precipitation) in fig. 4. The coprecipitation process was found to be extremely sensitive to pH, the Y:Ba:Cu ratio in the precipitate approaching 1:2:3 only at pH = 2.40 ± 0.05. The precipitate is Ba-deficient below this value and Cu-deficient above it [11]. It is not possible to control the pH *during* the reaction between microemulsions and only the initial pH of the reactants can be controlled. However, the microemulsion process was found to be less pH-sensitive. An initial reactant pH anywhere between 3.5 and 4.0 leads to a precipitate which yields monophasic YBCO on calcination.

4. Characterization of the oxide product

The microemulsion-derived oxalate precipitate converts to single-phase YBCO on calcining at 820°C for 2 h. The conventionally precipitated material required at least 860°C (6 h) for complete conversion to YBCO. The equivalent spherical diameter (ESD) of the particles of the dried oxalate precipitate and the calcined oxide were obtained from surface area measurements using the BET technique [12]. Table II shows that the microemulsion method yields appreciably smaller particles of the oxalate precipitate as well as the calcined oxide when compared to the conventional method. However, the microemulsion-derived YBCO powder (prepared at 820°C) does not exhibit Meissner effect down to 4 K, even after oxygen-annealing at 500°C. The conventionally pre-

Table II
Comparison of selected physical properties of $YBa_2Cu_3O_{7-x}$ prepared by conventional aqueous phase precipitation and microemulsion reaction.

	Microemulsion reaction	Conventional reaction
1. ESD of (Y, Ba, Cu) oxalate precipitate:	47.4 nm	380.6 nm
2. ESD of YBCO powder: Calcined at:	274.8 nm 820°C, 2 h	626.6 nm 860°C, 6 h
3. Grain size of YBCO pellet (from SEM): Sintered at:	15–50 μm 925°C, 12 h	0.5–2.0 μm 925°C, 12 h
4. Density of sintered pellet (fraction of single crystal density)	98(±3)%	90(±2)%
5. Magnetic susceptibility of Field-cooled sintered pellet (demagnetization corrected)	-10.95×10^{-3} (emu cm^{-3})	-3.06×10^{-3} (emu cm^{-3})
6. Magnetic susceptibility of Zero-Field-Cooled sintered pellet (demagnetization corrected)	-72.05×10^{-3} (emu cm^{-3})	-11.43×10^{-3} (emu cm^{-3})
7. Fraction of ideal Meissner signal ($-1/4\pi$)	90.5%	14.4%
8. Superconducting T_c	93 K	91 K

Note: ESD = Equivalent Spherical Diameter.

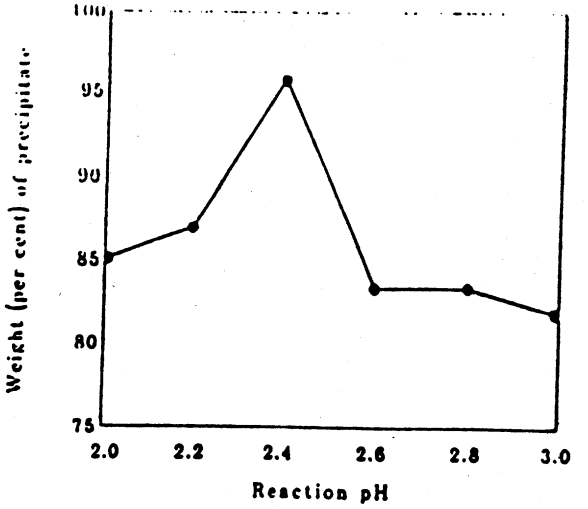

Fig. 4. Dependence of the weight of the oxalate precipitate on the pH of the reactants. The data refers to conventional aqueous phase reaction between (Y, Ba, Cu) nitrate and ammonium oxalate. The observed weights are normalized to the value expected for complete precipitation of all the cations.

cipitated microparticulate YBCO (calcined at 860 C) shows only a weak Meissner effect. The absence of superconductivity in the microemulsion-derived fine particle sample mets further discussion: (1) The X-ray diffraction (XRD) spectrum of the calcined YBCO powder does not show a clear orthorhombic split – and the tetragonal phase of YBCO is known to be nonsuperconducting. On the other hand, a small splitting may be masked by a particle-size induced broadening of the XRD lines. (2) The T_c for YBCO decreases with decreasing particle size [13] but the effect is appreciable only below about 120 nm. The ESD is larger (about 275 nm) in the present case. (3) The grain-boundary is essentially a defect region, and the large specific surface area of these samples may present a high concentration of flux-pinning centers.

The advantage of using the microparticulate precursors obtained from microemulsion becomes evident when the properties of the *sintered* material are compared. The calcined YBCO powder derived from the microemulsion (sample A) and the bulk aqueous phase (sample B) were both pressed into 3 mm diameter, 1 mm thick pellets (applied uniaxial pressure ≈ 1.2 GPa) and sintered under identical conditions: 925 C for 12 h. Neither sample was oxygen-annealed. Both the calcination and sintering steps were performed in air. The same cooldown program was used in both cases: T_{in}... (5°/min) → 500°C, held 0.5 h ... (2°/min) → 400°C, held 0.5 h ... (5°/min) → 200°C (T_{in} = calcination or sintering temperature, see table II). The superconducting transition temperature (as reported in table II) represents the temperature at which the susceptibility becomes negative.

The surface microstructure of the gold-coated sintered pellets (one of each derived from sample A and sample B) were observed under a scanning electron microscope (Jeol JSM-6400 and Jeol JSM-35C). Since the as-sintered surface of a pellet is not always a reliable indicator of the actual grain morphology, we also observed freshly cleaved surfaces from the sintered pellets. The SEM images of the as-sintered and cleaved surfaces (of the same pellet) were very similar. The microstructure of the two sintered pellets (samples A and B) were strikingly different. Sample A had much larger and more densely-packed grains than sample B (see fig. 5). This is consistent with the fact sample A had a very high bulk density (measured by the usual immersion procedure): about 98(±3)% of the corresponding single crystal value.

The temperature dependence of the DC susceptibility of the sintered pellets was measured down to 4.2 K under a field of 23 G. The microemulsion-derived material (sample A) exhibited substantially larger zero-field-cooled (diamagnetic shielding) and field-cooled (flux expulsion) signals (fig. 6). The demagnetization-corrected value of the low-field ZFC signal for sample A is 90% of the Meissner shielding expected from an ideal sample ($-1/4\pi$). The corresponding value for Sample B is only 14%. (This does not represent the best value obtainable from conventional methods, and it may be improved by oxygenation and optimization of sintering conditions.) The Meissner fraction is known to depend on the applied field [14]. The dependence is particularly strong for low fields and the Meissner fraction approaches 100% for fields in the region ≈ 0.1–0.01 G. Note, however, that the relatively high value (90%) that we obtained for the microemulsion-derived samples correspond to a comparatively large field (23 G).

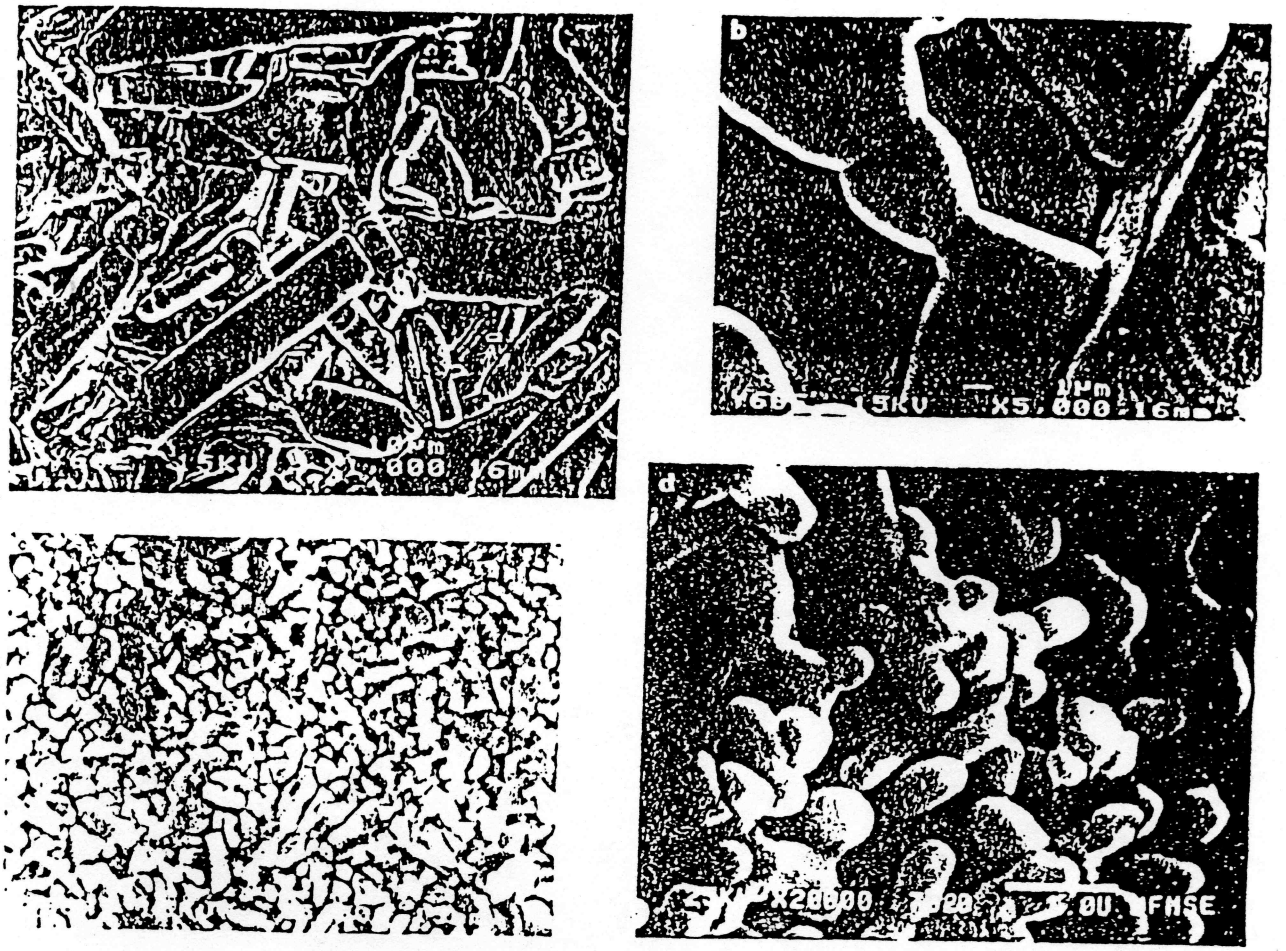

Fig. 5. Scanning electron micrographs showing the microstructure of the sintered $YBa_2Cu_3O_{7-x}$ pellets synthesized by the microemulsion-mediated reaction (a, b) and the conventional aqueous reaction (c, d). The magnifications used were: (a) 1000, (b) 5000, (c) 5000 and (d) 20 000.

5. Summary

We have shown that microemulsions provide a novel vehicle for the synthesis of a microparticulate oxalate precursor which yields very high density sintered pellets of $YBa_2Cu_3O_{7-x}$ and shows a strong Meissner signal. Perfect chemical homogeneity is ensured by the extremely small size of the reaction vehicle (≈ 13 nm). Optimization of the sintering conditions should produce better quality ceramic material, presumably with a high critical current density. Since the microemulsion droplets are monodisperse and their size can be controlled to a certain extent, this method may be used for producing fine particle (in the range ≤ 100 nm) oxide superconductors with a narrow size distribution. Such material would be useful for studying the grain-size dependence of various superconductive parameters. On the other hand, this is the first application of the microemulsion technique to the production of complex (multicationic) oxides. This method should be particularly useful for the preparation of other materials where an accurate maintenance of stoichiometry is crucial.

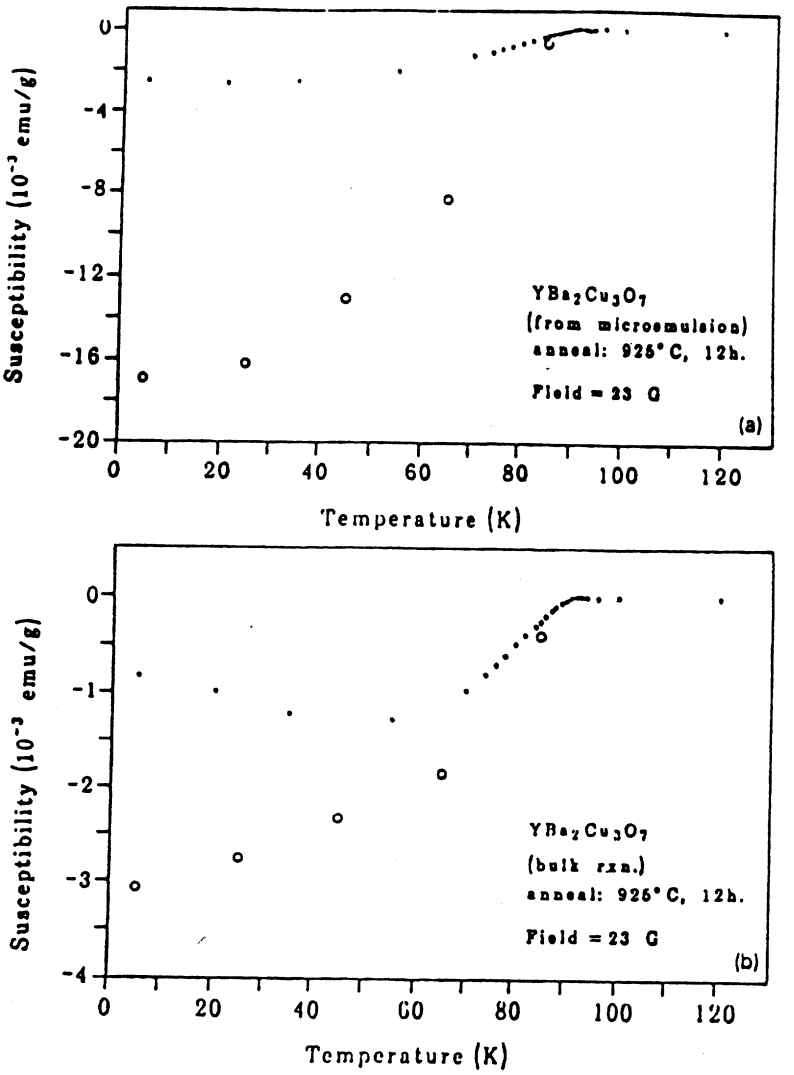

Fig. 6. Temperature dependence of the low-field (23 G) DC susceptibility for sintered $YBa_2Cu_3O_{7-x}$ pellets synthesized by (a) microemulsion-mediated reaction and (b) conventional aqueous reactions. Zero-field-cooled and field-cooled branches are indicated by open and closed circles, respectively.

Acknowledgements

We acknowledge the support provided by the Defense Advanced Research Project Agency and the National Science Foundation. We also thank Prof. G. Stewart and his colleagues for their help with susceptibility measurements. One of us (P.A.) wishes to thank P. Guptasarma, M.S. Multani and V.R. Palkar for their suggestions.

References

[1] P.G. DeGennes and C. Taupin, J. Phys. Chem. 86 (1982) 2294.
[2] Microemulsion and Related Systems, eds. M. Bourrel and R.S. Schechter (Marcel Dekker, New York, 1988).
[3] M. Boutonnet, J. Kizling, P. Stenius and G. Maire, Colloids and Surfaces 5 (1982) 209.
[4] S. Bandow, K. Kimura, K. Kon-no and A. Kitahara, Jpn. J. Appl. Phys. 26 (1987) 713.

[5] M.J. Hou and D.O. Shah, in: Interfacial Phenomena in Biotechnology and Materials Processing, eds. Y.A. Attia et al. (Elsevier, Amsterdam, 1988) p. 443.
[6] P. Ayyub, M. Multani, M. Barma, V.R. Palkar and R. Vijayaraghavan, J. Phys. C. 21 (1988) 2229.
[7] S.A. Safran, G.S. Grest and A.L.R. Bug, in: Microemulsion Systems, eds. H.L. Rosano and M. Clausse (Marcel Dekker, New York, 1987) p. 235.
[8] P. Ayyub and D.O. Shah, in preparation.
[9] see, for example: Light Scattering in Liquids and Macromolecular Solutions, eds. V. Degiorgio, M. Corti and M. Giglio (Plenum, New York, 1980).
[10] H.F. Eicke, J.C.W. Shepherd and A. Steinemann, J. Colloid Interface Sci. 56 (1976) 168.
[11] F. Caillaud, J. Baumard and A. Smith, Mater. Res. Bull. 23 (1988) 1273.
[12] see, for example: Particle size Measurements, ed. T. Allen (Chapman and Hall, London, 1974).
[13] M.S. Multani, P. Guptasarma, V.R. Palkar, P. Ayyub and A.V. Gurjar, Phys. Lett. A 142 (1989) 293.
[14] L. Krusin-Elbaum, A.P. Malozemoff, Y. Yeshurun, D.C. Gronemeyer and F. Holtzberg, Physica C 153–155 (1988) 1469.